



Chemistry A European Journal

 **Chemistry
Europe**
European Chemical
Societies Publishing

Accepted Article

Title: Meso and β -Pyrrole Linked Chlorin-Bacteriochlorin Dyads for Promoting Far-Red FRET and Singlet Oxygen Production

Authors: Francis D'Souza, M. Dukh, W.A. Tabaczynski, S. Seetharaman, Z. Ou, K. M. Kadish, and R. Pandey

This manuscript has been accepted after peer review and appears as an Accepted Article online prior to editing, proofing, and formal publication of the final Version of Record (VoR). This work is currently citable by using the Digital Object Identifier (DOI) given below. The VoR will be published online in Early View as soon as possible and may be different to this Accepted Article as a result of editing. Readers should obtain the VoR from the journal website shown below when it is published to ensure accuracy of information. The authors are responsible for the content of this Accepted Article.

To be cited as: *Chem. Eur. J.* 10.1002/chem.202003042

Link to VoR: <https://doi.org/10.1002/chem.202003042>

WILEY-VCH

Meso and β -Pyrrole Linked Chlorin-Bacteriochlorin Dyads for Promoting Far-Red FRET and Singlet Oxygen Production

Mykhaylo Dukh,^[a] Walter A. Tabaczynski^[a], Sairaman Seetharaman,^[b] Zhongping Ou,^[c] Karl M. Kadish,^{*,[c]} Francis D'Souza,^{*,[b]} Ravindra K. Pandey^{*,[a]}

Abstract: A series of chlorin-bacteriochlorin dyads (derived from naturally occurring chlorophyll-a and bacteriochlorophyll-a), covalently connected either through the meso-aryl or β -pyrrole position (position-3) via an ester linkage have been synthesized and characterized as a new class of far-red emitting fluorescence resonance energy transfer (FRET) imaging, and heavy atom lacking singlet oxygen producing agents. From systematic absorption, fluorescence, electrochemical and computational studies, the role of chlorin as an energy donor and bacteriochlorin as an energy acceptor in

these wide-band capturing dyads was established. Efficiency of FRET evaluated from spectral overlap was found to be 95% and 98% for the meso-linked and β -pyrrole linked dyads, respectively. Furthermore, evidence for the occurrence of FRET from singlet-excited chlorin to bacteriochlorin was secured from studies involving femtosecond transient absorption studies in toluene. The measured FRET rate constants, k_{FRET} , were on the order of 10^{11} s^{-1} , suggesting the occurrence of ultrafast energy transfer in these dyads. Nanosecond transient absorption studies confirmed relaxation of the energy transfer product,

$^1\text{Bchl}^*$, to its triplet state, $^3\text{Bchl}^*$. The $^3\text{Bchl}^*$ thus generated was capable of producing singlet oxygen with quantum yields comparable to their monomeric entities. The occurrence of efficient FRET emitting in the far-red region and the ability to produce singlet oxygen make the present series of dyads useful for photonic, imaging and therapy applications.

Keywords: Chlorin, Bacteriochlorin, Far-infrared FRET, Singlet Oxygen Production, Ultrafast spectroscopy

Introduction

There is a growing demand for photosensitizer probes capable of emitting in the far-red region^[1] due to their useful applications in the areas of photovoltaics, optoelectronics, photodynamic therapy (PDT), and non-invasive optical bio-imaging.^[2-6] In bio-imaging, a successful probe should exhibit strong absorption and emission in the red- or far-red regions, have well-defined absorption and emission bands exhibiting large Stokes shift, possess a sufficiently long-lived excited state and exhibit high photostability.^[7] The far-red probes have valuable advantages of deeper tissue penetration and significantly lower background emission and scattering compared to visible wavelength emitting probes.^[8-9] A large absorption-fluorescence spacing (Stokes shift) facilitates the ability to prevent scattered excitation light from reaching the fluorescence detection systems, leading to diminishing of the image quality. Rigorous studies over the last two decades have resulted in the development of fluorescent probes with properties desirable for *in vivo* therapeutic and imaging applications.^[2-9] However, the development of such far-red probes, including the widely utilized cyanine dyes, demand tedious synthesis accompanied by low reaction yields, limited solubility and low photostability.

An elegant approach to increase the Stokes shift of fluorescent probes is to build donor-acceptor dyads capable of undergoing fluorescence resonance energy transfer (FRET).^[10] These dyads are comprised of an energy donor which is covalently linked to an energy acceptor. Excitation of the donor at absorption maxima far from emission maxima of the acceptor for obtaining a large Stokes shift could promote ultrafast energy transfer to the acceptor. Additionally, in the construction of such dyads the utilization of a far-red emitting fluorophore as an energy acceptor offers the benefit of far-red imaging. Thus, such dyads would behave as single fluorophores with a very large Stokes shift highly desired for far-red imaging. Another useful property of these dyad-sensitizers would be in their ability to produce singlet oxygen needed for PDT therapeutic applications.^[7] A sufficiently higher triplet state energy of the acceptor as compared to the energy of singlet oxygen is the main requirement to observe singlet oxygen.^[11]

Chlorins (Chl) and bacteriochlorins (Bchl), core macrocycles in naturally occurring photosynthetic pigments, are tetrapyrrole macrocycles with one and two reduced carbon-carbon double bonds, respectively.^[12] The progressive reduction of double bonds results in an enhancement of absorption and emission in the red region for chlorins (600-700 nm range) and in the far-red for bacteriochlorins (715-800 nm). Although naturally occurring chlorins and bacteriochlorins have been used in bioimaging, they often encounter issues related to difficulties associated with synthetic modifications and facile oxidation to yield the corresponding chlorins and porphyrins, respectively.^[13] Lindsey and co-workers have reported *de novo* synthetic methods for obtaining stable chlorins and bacteriochlorins by incorporation of germinal methyl substituents at the pyrrole ring macrocycles, preventing oxidation.^[14] Furthermore, these authors were successful in synthesizing

[a] Dr. M. Dukh, Dr. W. A. Tabaczynski, Prof. Dr. R. K. Pandey, PDT Center, Cell Stress Biology, Roswell Park Cancer Institute, Buffalo, NY 14263, USA. E-mail: ravindra.pandey@roswellpark.org

[b] S. Seetharaman, Prof. Dr. F. D'Souza, Department of Chemistry, University of North Texas, 1155 Union Circle, #305070, Denton, TX 76203-5017 (USA); E-mail: Francis.DSouza@UNT.edu

[c] Dr. Z. Ou, Prof. Dr. K. M. Kadish, Department of Chemistry, University of Houston, Houston, TX 77204, E-mail: kadish@central.uh.edu

Supporting information for this article, complete synthesis and characterization details,

covalently linked chlorin-bacteriochlorin dyads for subsequent FRET and far red bioimaging.^[9a]

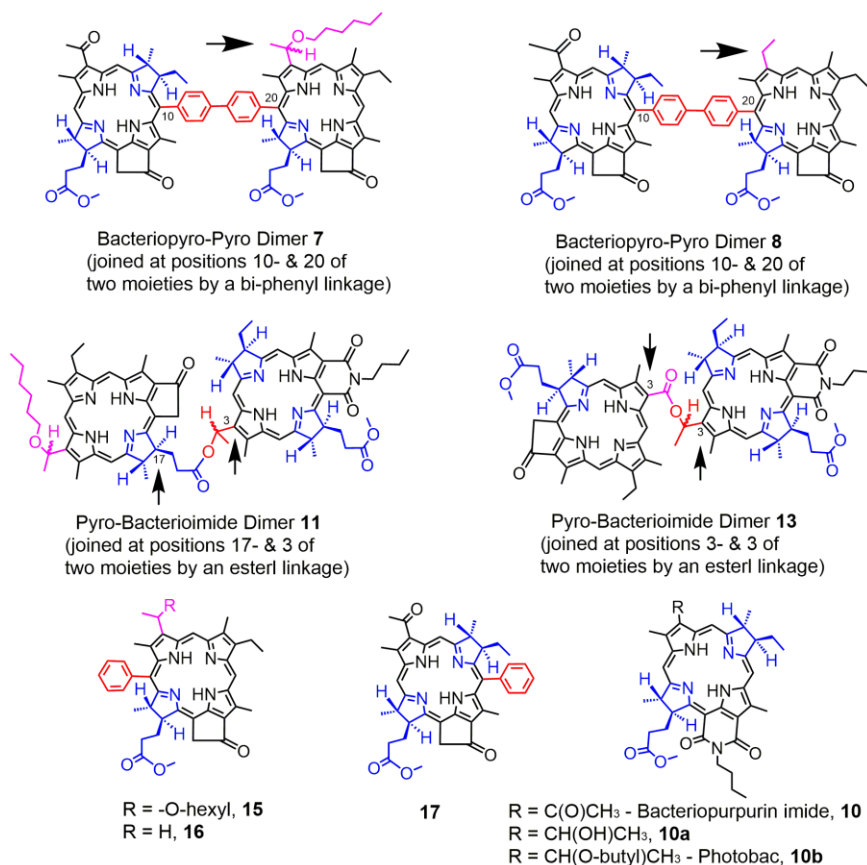


Figure 1. Structures and abbreviations of dimers and monomers investigated for FRET and singlet oxygen generation in the present study.

In the present study, we have modified both chlorins and bacteriochlorins^[15] and successfully synthesized four new dyads (see Figure 1 for structures). These dyads are connected either through the meso-aryl groups (dyads **7** and **8**) or β -pyrrole **11** (monomers are linked at positions 17 and 3), and **13** (monomers are linked at position-3) via ester linkages. Systematic studies are then performed to probe FRET in these dyads in nonpolar toluene using a combination of spectral, electrochemical, and photochemical measurements. The kinetics of FRET, k_{FRET} , in these dyads is also evaluated from femtosecond transient absorption (fs-TA) spectral studies. The ability of these dyads to produce singlet oxygen is also investigated and the results of our investigation show that the Chl-Bchl dyads developed here can function as probes for imaging modalities and therapeutic agents for PDT applications.

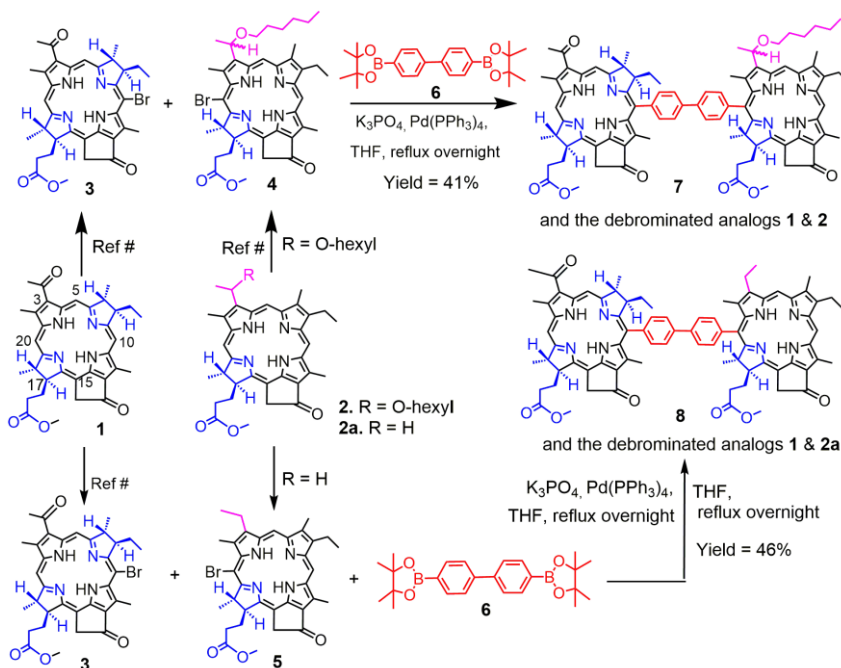
Results and Discussion

Syntheses

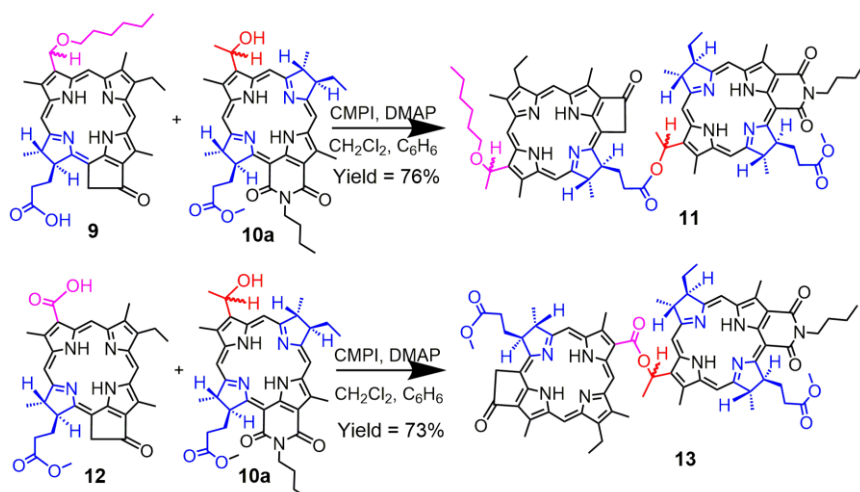
Two different synthetic strategies were followed for the preparation of Chl-Bchl dyads with a diphenyl linkage (Scheme 1) or with an ester linkage (Scheme 2). For synthesis of the unsymmetrical dyads **7** and **8**, methyl 3-acetyl bacteriopyropheophorbide **1** was obtained from *Rhodospira rubra*,^[16] which on reacting with N-bromosuccinimide (NBS) gave the corresponding 10-bromo analog **3** in 66% yield by

following our previously reported methodology.^[17] The chlorins **2** [methyl-3-(1'-hexyloxy)ethyl-3-devinylpyropheophorbide-a]^[18] and **2a** [methyl-3-ethyl-3-devinylpyropheophorbide-a], differing only in the functional group at position-3, were reacted individually with pyridinium tribromide to give the respective 20-bromo analogs **4** and **5** which were isolated in 87% yield.^[17] Reaction of the 10-bromobacteriochlorin **3** with the 20-bromo chlorins **4** and **5** in presence **6** under Suzuki reaction conditions^[19, 20] afforded the desired Chl-Bchl dyads **7** and **8** in 41% and 46%, yield, respectively, along with the debrominated analogs **1**, **2** and **2a** in 30-35% yield (Scheme 1).

For synthesis of the dyads with ester linkages, the methyl ester functionality in chlorin **2** was hydrolyzed with lithium hydroxide (LiOH)/water^[21] and the resulting product **9** obtained in quantitative yield was reacted with 3-(1'-hydroxyethyl)-3-deacetyl-bacteriopurpurin-18-N-butylimide methyl ester **10a** obtained by sodium borohydride reduction^[22] of the corresponding 3-acetyl analog **10** in the presence of 2-chloro-1-methylpyridinium iodide (CMPI) and 4-(dimethylamino)pyridine (DMAP) at room temperature for 2 hours (Scheme 2) and the desired dyad **11** linked at position-17 of the chlorin and position-3 of the bacteriochlorin with an ester linkage was isolated in 76% yield. Following similar reaction conditions, the Chl-Bchl dyad **13** was obtained in 73% yield by reacting methyl 3-carboxyl-3-devinyl-pyropheophorbide-a **12** with **10a**. To further determine the photophysical properties of the monomers vs the unsymmetrical dyads, the 20-phenyl substituted

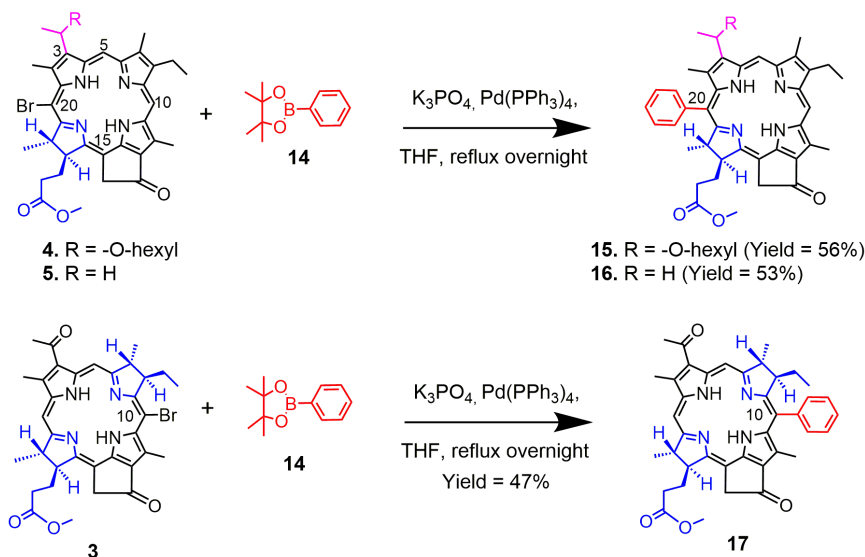


Scheme 1. Synthesis of bacteriochlorin-chlorin dimers linked at the meso-positions by a diphenyl bridge.



Scheme 2. Synthesis of bacteriochlorin-chlorin dimers linked at positions 17-3 and at positions 3-3 of the two moieties.

chlorins **15**, **16** and 10-phenyl substituted bacteriochlorin **17** as model compounds were also synthesized by following the methodology depicted in **Scheme 3**.



Scheme 3: Synthesis of 20-phenyl- methyl pyropheophorbide and 10-phenyl-methyl bacterio-phyropheophorbide analogs.

NMR spectral characterization

The ^1H and ^{13}C NMR (1D and 2D), of each intermediate monomer and dyad were generally consistent with the proposed structures (see the SI for a detailed synthesis of the compounds, characterization by UV-vis, HRMS, NMR analyses and ^1H and ^{13}C NMR spectra of the dimers, Figures S1-S14). Spectral features exhibited by most of these compounds are similar to those observed for known compounds of similar structure. However, selected protons of the dyads **11** and **13** show significant differences in the ^1H chemical shifts relative to the corresponding, unsubstituted (i.e. monomeric) photosensitizers. The Chl-Bchl dyad **11** exhibits chemical shift differences ($\Delta\delta$'s) for several protons in the A- and B-ring regions of the bacteriochlorin moiety, relative to δ values observed for a similar analog 3-(1'-butyloxy)ethyl-bacteriopurpurin-18-N-butylimide (Photobac, **10b**) reported from our laboratory.^[22] The largest $\Delta\delta$ is for 3^1-H , which exhibits a deshielding of 1.4 ppm, relative to Photobac, **10b**. The 7-CH_3 protons are shielded by up to ~ 0.7 ppm relative to Photobac, **10b**. In this case, however, the

shielding depends upon the diastereomeric form observed. Two of the four stereoisomers exhibit shieldings of only ~ 0.1 ppm for 7-CH_3 . Small to moderate shieldings are observed for 5-H (0.4 ppm), 7-H (0.3 ppm) and 8-H (0.1 or 0.4 ppm, depending upon the stereoisomeric form). In contrast, the chlorin moiety of dimer **11** shows no significant differences in proton chemical shift relative to the monomer **2**.^[18]

The Chl-Bchl dyad **13** (linked through position-3 substituents of both macrocycles) exhibits chemical shift differences for several protons in the A- and B-ring regions of both the moieties, relative to δ values observed for the corresponding monomer **12** (methyl-3-carboxypyro-3-devinyl-pyropheophorbide-a)^[23] and Photobac, **10b**. The pyro-moiety exhibits small to moderate $\Delta\delta$'s for 5-H (0.2/0.3 ppm shielding), 7-CH_3 (0.2/0.4 ppm deshielding), and 10-H (0.2/0.3 ppm shielding), where slashes (/) separate $\Delta\delta$'s observed for different diastereomers.

The bacteriopurpurinimide moiety of **13** exhibits large $\Delta\delta$'s (relative to Photobac, **10b**) for 3^1-H , 3^1-CH_3 , and 7-CH_3 . The 3^1-H and 3^1-CH_3 protons are deshielded by 2.2 and 0.7 ppm, respectively. The 7-CH_3 signal was shielded by up to ~ 0.8 ppm in some diastereomers, while in other forms 7-CH_3 exhibits only a very small shielding (< 0.1 ppm). Several additional small-to moderate-sized shift differences are observed (relative to Photobac, **10b**) for the bacteriopurpurinimide moiety. Deshieldings are observed for 2-CH_3 (0.4 ppm), 5-H (0.3 ppm) and 20-H (0.2 ppm), while shieldings are observed for 7-H (0.1/0.3 ppm), 8-H (0.1/0.2 ppm), and $8\text{-CH}_2\text{CH}_3$ (0.1/0.4 ppm). The $\Delta\delta$'s noted above could arise from a number of different sources, but the spatial distribution of the groups exhibiting these shift differences suggests they are caused by interaction between the two different photosensitizer moieties in each dyad. The large deshieldings observed for the 3^1-H and 3^1-CH_3 protons of the bacteriopurpurinimide moiety in both **11** and **13** may be due to basic structural differences between these dyads and the monomers. The data suggest that the ester linker joining the two moieties introduces significant changes to the electronic environment of the 3-position substituents relative to the O-butyl group found in Photobac, **10b** (monomer).

Other protons showing significant $\Delta\delta$'s are all located in the vicinity of the A- and B-rings. Their chemical shifts may be influenced by structural elements located in the neighboring photosensitizer (i.e. the other "half" of the dyad). These elements may be functional groups such as the ester linker, or the keto group at position-13¹ of the pyropheophorbide-a analog. Ring current effects could also be responsible for the observed $\Delta\delta$'s. A close proximity of any of the shifted groups to the π -systems of the neighboring aromatic macrocycle might also induce the observed shieldings/deshieldings. The notable $\Delta\delta$'s observed in **11** are fewer and less widespread than those seen in **13**. This may be due to differences in linker length and flexibility. Dyad **11** contains a longer and presumably more flexible linker than **13**. Longer linker length means the two photosensitizers in **11** can assume positions that are farther apart than is possible in **13**. Both the longer linker

length and greater flexibility in **11** allow greater conformational freedom as compared with **13**. Thus, it may be less likely that **11** adopts a conformation resulting in a close approach of its two photosensitizers. However, a few significant $\Delta\delta$'s were observed in **11** suggesting some degree of interaction.

UV-vis and fluorescence studies: Evidence of FRET

Figure 2 shows the visible and far-red absorption and fluorescence spectra of dyads **7** and **11** along with the corresponding control Chl monomer **2** and Bchl monomers **17** or **10** while Figure S15 details spectra of the dyads **8** and **13** along with the corresponding control monomers. The peak maxima, fluorescence quantum yields and lifetimes, and excited singlet state energies are summarized in Table 1. Appreciable changes can be noted between the absorption and emission spectrum of meso-aryl and β -pyrrole substituted control monomers and the corresponding dyads. For example, the meso-aryl substituted chlorin **15** revealed an intense Soret band at 416 nm with shoulder peaks at 323 and 378 nm along with four peaks in the visible region at 514, 546, 614 and 671 nm. The 671 nm peak was the most intense among the visible peaks due to reduced symmetry, resulting from the one reduced carbon-carbon double bond. In the

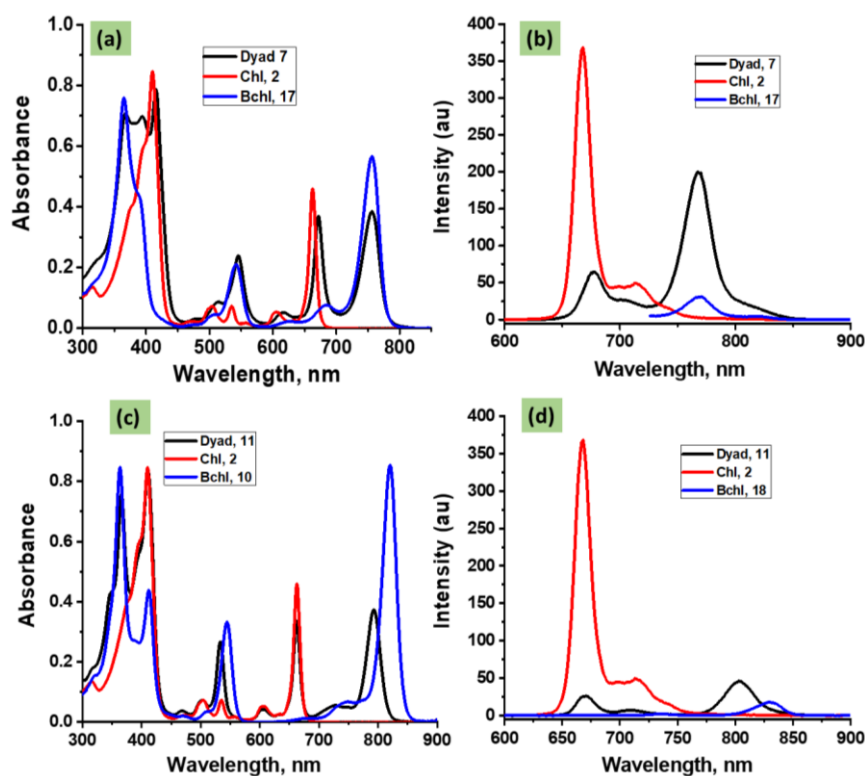


Figure 2. Absorption and fluorescence spectra of the dyads **7** and **11** along with the control chlorin **2** and bacteriochlorin **17** or **10**, in toluene. The samples were excited at 415 nm corresponding to chlorin Soret peak maxima.

case of meso-aryl substituted bacteriochlorin **17**, the Soret band was located at 366 nm with the shoulder peak at 387 nm, while the visible peaks were at 542, 632, 684 and 757 nm. The low energy visible band was the most intense owing to the presence of two reduced carbon-carbon double bonds. The spectra of the dyads **7** and **8** with a diphenyl linker at the meso-positions is a simple addition of the spectrum of the monomers, suggesting minimal intramolecular interactions between the two entities (see Figures 2a and S15a). The Soret band of the dyad **7** revealed three distinct

peak maxima at 368, 396 and 416 nm while in the visible region peaks were observed at 512, 544, 633, 667 and 757 nm.

The fluorescence maxima for Chl monomer **2** was located at 668 and 715 nm while for Bchl monomer **17** the main peak was at 769 nm (Figure 2b). When the fluorescence spectrum of the dyad **7** was recorded at the excitation wavelength of 415 nm corresponding to the Chl Soret band; the Chl emission was found to be highly quenched as compared to its original intensity with the appearance of a Bchl emission at 769 nm. The intensity of the 769 nm peak was found to be almost twice that obtained for an equimolar mixture of Chl and Bchl monomers at the excitation wavelength of 415 nm. These results suggest the occurrence of singlet-singlet energy transfer in the dyad **7**. The excitation spectrum recorded for the dyad by holding the emission monochromator to 769 nm, the wavelength corresponding to Bchl emission maxima in the dyad, and scanning the excitation wavelength revealed peaks corresponding to both Chl and Bchl monomer entities, thus confirming the occurrence of an excitation process.^[10]

Similar observations were also made for the second meso-linked dyad **8** where the absorption spectrum was a simple addition of spectra for the corresponding chlorin and bacteriochlorin monomeric entities (Figure S15a). Importantly, the occurrence of singlet-singlet energy transfer from $^1\text{Chl}^*$ to Bchl was confirmed from fluorescence emission and excitation spectral studies (see Figure S15b and S16).

Contrary to the meso-linked dyads, the β -pyrrole linked dyads revealed significant spectral changes in terms of both absorption and emission peak maxima as compared to their control monomers, thus suggesting the occurrence of intramolecular interactions between the entities (see Figures 2c and S15c). For example, the absorption peak maxima of the Chl monomer **2** are located at 316, 410, 505, 535, 605 and 664 nm while in the case of the Bchl monomer **10**, these peaks are at 364, 414, 470, 544, 750 and 820 nm. As expected for Chl and Bchl derivatives, the low energy visible band revealed the highest intensity. The fluorescence peak maxima of **2** are located at 668 and 715 nm while for **10b**, the emission peak maximum is located at 830 nm. When these two monomers are covalently linked via an ester linked through the β -pyrrole position to form the dyad **11**, significant spectral changes can be noticed and peak maxima are seen at 365, 410, 503, 533, 605, 662, 727 and 792 nm. The low energy peak at 820 nm in the bacteriochlorophyll monomer is blue-shifted to 792 nm in the dyad. When the chlorin entity in the dyad **11** was excited, the chlorin emission was found to be highly quenched with the appearance of a new peak at 804 nm corresponding to bacteriochlorin emission, thus suggesting the occurrence of singlet-singlet energy transfer in the dyad. The blue-shifted peak maxima in the dyad indicate appreciable interactions between the entities within the dyad. The excitation spectrum recorded for this dyad also support the energy transfer phenomenon (Figure S16). Similar observations can be made in the second β -pyrrole linked dyad, **13**, wherein spectral evidence for intramolecular interactions between the individual entities and efficient singlet-singlet energy transfer is seen (see Figure S15c and d).

As shown in Table 1, the lifetime of control Chl monomers (**2**, **15** and **16**) are in the range of 7-7.5 ns while in the Bchl monomers (**17** and **10**) it was 1.6-1.9 ns, largely tracking the fluorescence quantum yields. In the case of the dyads, we could only measure the lifetime corresponding to the Bchl and not Chl as it was highly quenched. The singlet energy $E_{0,0}$ calculated from the mid-point of 0,0 transitions of absorption and fluorescence peak maxima is ~1.85 eV for $^1\text{Chl}^*$ and 1.5-1.6 eV for $^1\text{Bchl}^*$, respectively. Energies for $^3\text{Chl}^*$ and $^3\text{Bchl}^*$ were taken from the literature,^[24] being 1.3 eV for $^3\text{Chl}^*$ and 1.2 eV for $^3\text{Bchl}^*$.

Table 1. Optical absorption and fluorescence emission data of the investigated compounds (see Figure 1 for structures) in toluene.

Compound	Absorption, nm	Fluorescence, nm	Φ_F^a	τ , ns	$E_{0,0}$	
Monomer	2	316, 410, 505, 535, 605, 664	668, 715	0.162	7.47	1.86
	16	416, 511, 543, 612, 668	673, 718	0.141	7.0	1.85
	15	323, 378, 416, 478, 514, 546, 614, 671	677, 725	0.152	7.43	1.84
	10	364, 414, 470, 544, 750, 820	830	0.015	1.59	1.50
	17	366, 387, 542, 632, 684, 757	769	0.0023	1.87	1.63
Dyad	11	365, 410, 503, 533, 605, 662, 727, 792	668, 804	--	7.00	1.55
	13	366, 415, 470, 532, 625, 685, 728, 794	696, 804	--	6.30	1.56
	7	368, 396, 416, 512, 544, 633, 667, 757	673, 769	--	6.73	1.63
	8	367, 394, 415, 416, 514, 546, 614, 672, 756	678, 766	--	6.89	1.64

^a-See Ref. 25 and 26

The dyads were also geometry optimized by PM3 optimization methods to check whether steric interactions exist between the entities, and also to evaluate the intramolecular distances between the two entities as shown in Figure S17. No noticeable steric crowding was observed in any of the dyads. The edge-to-edge distance between the entities was found to be ~11 Å for the β -pyrrole linked dyads and ~16 Å for the meso linked dyads.

To strengthen our understanding of the FRET process,^[27] the spectral overlap integral involving emission of the donor and absorption of the acceptor was evaluated by using software provided by FluoTools,^[28] while the FRET efficiency, E , was estimated from equation 1^[10].

$$E = 1 - (I_{D-A}/I_D) \quad (1)$$

where I_{D-A} and I_D represent fluorescence intensities of the donor-acceptor dyad and the donor, respectively. The estimated values are given in Table 2. For the meso-substituted dyads **7** and **8** the FRET efficiency was in the range of 94-96% while for the β -pyrrole derivatized dyads it was 97-98%, meaning a very high energy transfer efficiency in these dyads. The improved efficiency in the

latter type of dyads could easily be attributed to a better spectral overlap and shorter distance between the donor and acceptor entities.

Table 2. Spectral overlap integral, J , FRET efficiency, Φ_{FRET} , and rate of energy transfer, k_{FRET} , for the investigated dyads in toluene.

Dyad	J , cm^4/M	Φ_{FRET}	k_{FRET} , s^{-1}
7	1.19×10^{-15}	0.94	1.7×10^{11}
8	1.11×10^{-15}	0.96	1.7×10^{11}
11	1.48×10^{-14}	0.98	0.6×10^{11}
13	1.72×10^{-14}	0.97	2.1×10^{11}

Electrochemical and spectroelectrochemical studies

Although the dyads synthesized in the present study were primarily targeted for FRET studies, it was required to study their electrochemical behavior since some of them revealed appreciable intramolecular type interactions. Figure 3 shows cyclic voltammograms of the four dyads revealing the first two oxidations and first two reductions while voltammograms of the dimers scanned to full potential window of the solvent, and those of monomeric precursors are shown in Figures S18 and S19 in SI. The Chl and BChl derivatives both undergo two one-electron oxidations and two one-electron reductions within the potential window of the solvent. In the case of dyads, four oxidations and four reductions are observed in which the first two oxidations and first two reductions were fully reversible. The measured redox potentials are listed in Table 3.

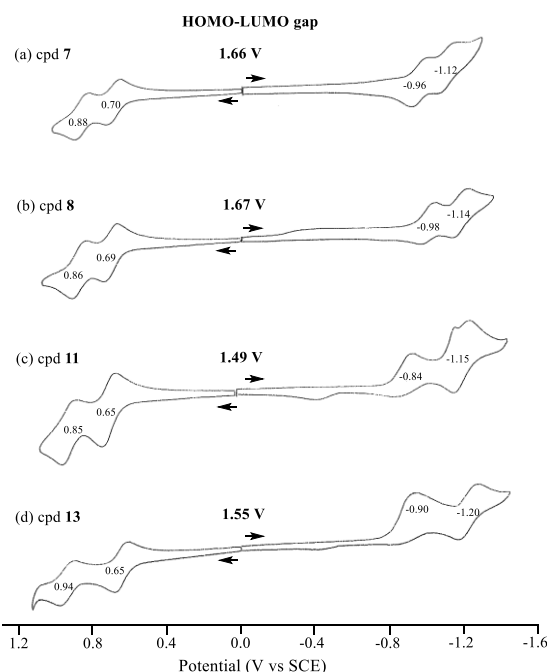


Figure 3. Cyclic voltammograms of the indicated compounds in CH_2Cl_2 containing 0.1 M (TBA)ClO₄. Scan rate = 100 mV/s.

An examination of the data in Table 3 reveals the following: (i) The monomeric Chl derivatives **2**, **15** and **16** are harder to oxidize and harder reduce than the monomeric Bchl derivatives **17** and **10** resulting in a larger HOMO-LUMO gap. (ii) The optical HOMO-LUMO gap ($E_{0,0}$) is slightly higher for the Chl derivatives

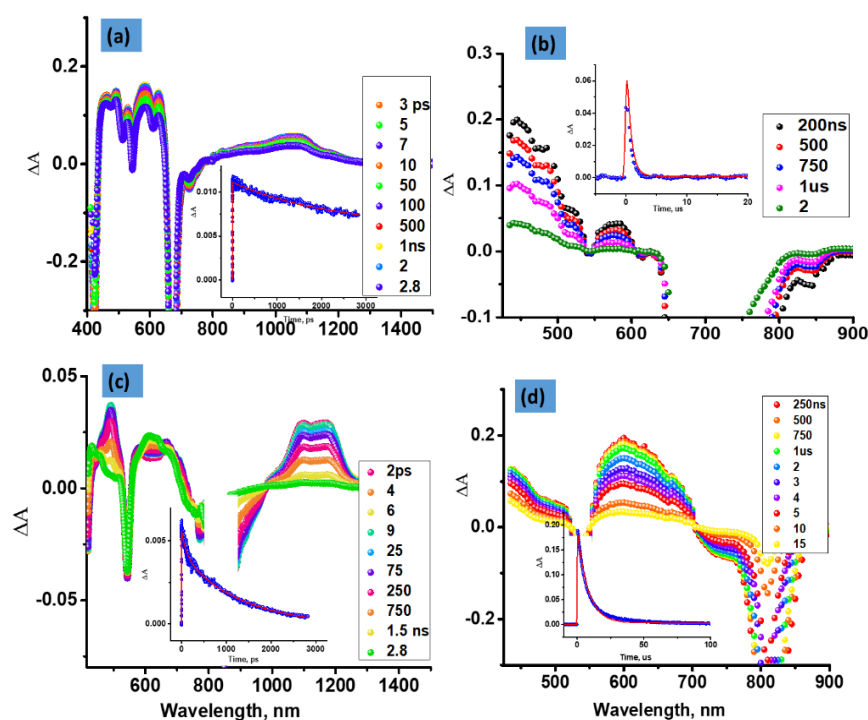


Figure 5. fs-TA spectra (a and c) and ns-TA spectra (b and d) at the indicated delay times of Chl **16** (a and c) and Bchl **10** (b and d) in toluene. The decay time profile of the far-red peak corresponding to singlet excited state transition, and decay time profile of the triplet peak are given as figure insets. The samples were excited at 670 nm for **16**, and at 820 nm for **10** during fs-TA measurements. For ns-TA studies the samples were excited at 415 nm.

Although spectral features corresponding to ESA, GSB and SE transitions could be readily identified from fs-TA spectra of the Bchl derivatives, their peak positions were much different from that observed in the case of Chl derivatives. For example, in the case of Bchl **10**, ESA peaks were located at 492, 668, 1095 and 1172 nm while negative peaks corresponding to GSB were located at 420, 545, and 772 nm, and SE emission at 830 nm (see Figure 5c). The decay and recovery of the positive and negative peaks were associated with a new set of peaks with maxima at 426 and 612 nm (see Figure 5c). The ns-TA spectral studies confirmed this to be due to $^3\text{Bchl}^*$ formation (Figure 5d). The $^3\text{Bchl}^*$ thus formed lasted for about 9.6 μs (Figure 5d inset for decay time profile). In the case of Bchl, **17** a similar spectral trend was observed with transient peak positions close to that observed for **18** due to structural similarity (Figure S21c and d). The $^3\text{Chl}^*$ lasted for about 5.6 μs (Figure S6d inset). These studies show successful population of the singlet excited state of both Chl and Bchl upon excitation followed by them undergoing ISC to populate respective triplet excited states that last for a few μs in toluene.

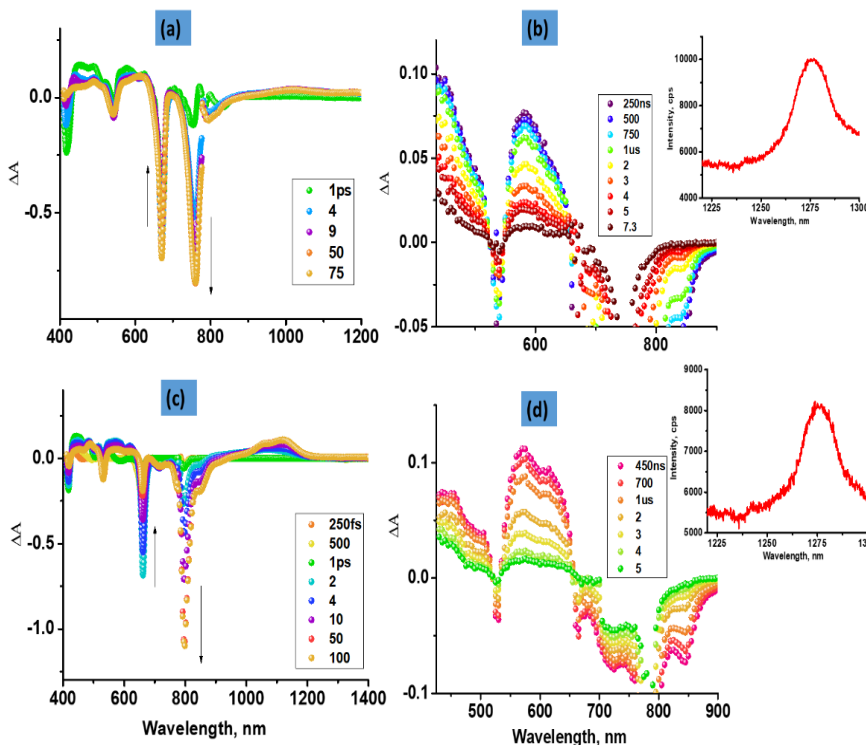


Figure 6. fs-TA at the indicated delay times (a and c), ns-TA at the indicated time intervals (b and d), and photoluminescence spectrum of generated singlet oxygen (inset of b and d) of (a) dyad **8**, and (b) dyad **11** in toluene. The samples were excited at a wavelength corresponding to Chl visible peak. For ns-TA studies the samples were excited at 415 nm.

Fs-TA and ns-TA spectral studies were then performed on the dyads and the spectral data are shown in Figures 6 and S22. Clear evidence of FRET from $^1\text{Chl}^*$ to Bchl in all of the dyads was seen. For example, in the case of the dyad, **8**, excitation at 757 nm corresponding to Chl absorption revealed instantaneous population of $^1\text{Chl}^*$ with positive peaks at 490, 582, 625, 700 and 1025 nm due to ESA (Figure 6a). This was also accompanied by negative peaks at 422, 541, and 667 nm due to GSB and SE. Rapid recovery of the positive and negative peaks was accompanied by new transient signal at 490, 612, 684 and 1020 nm and negative signals at 541 and 764 nm (Figure 6a). The remainder of the dyads followed a similar spectral trend, that is, rapid recovery of the transient peaks corresponding to the initially formed $^1\text{Chl}^*$ to populate $^1\text{Bchl}^*$ due to the FRET process (see Figures 6b and S22a and b). From the decay time constant of $^1\text{Chl}^*$ and lifetime of the corresponding Chl, the rates of FRET, k_{FRET} , were estimated and are tabulated in Table 2. A magnitude of $k_{\text{FRET}} \sim 10^{11} \text{ s}^{-1}$ suggest an ultrafast FRET process in these dyads.

In order to ascertain that the product of energy transfer Chl- $^1\text{Bchl}^*$ indeed populates the triplet excited state to yield Chl- $^3\text{Bchl}^*$, ns-TA spectral studies were performed. As shown in Figures 6b and d, and Figures S22b and d, all of the dyads revealed peaks corresponding to $^3\text{Bchl}^*$. The time constants for $^3\text{Bchl}^*$ decay was found to be 5.6 μs for **7**, 2.3 μs **8**, 2.5 μs **11** and 5.8 μs for **13**, slightly lower than that observed for monomeric Bchl derivatives.

Singlet oxygen production

Finally, the ability of the monomeric Chl and Bchl derivatives and the dyads to produce singlet oxygen was performed (see Figure 6 and S22 insets for photoluminescence spectra of singlet oxygen). As the triplet energies of both $^3\text{Chl}^*$ and $^3\text{Bchl}^*$ in the monomers, and the final photoproduct of the dyads, $^3\text{Bchl}^*$, are all higher than that of singlet oxygen, enabling derivatives to produce singlet oxygen in toluene. The quantum yields calculated with reference to zinc tetraphenylporphyrin (ZnTPP) are listed in Table 4. It is worthy to note that the quantum yields of singlet oxygen production from the dyads are comparable to that of the monomeric entities, a key feature for their photodynamic therapy applications.

Table 4. Quantum yields of singlet oxygen production by the dyads and control monomers in toluene.

Compound ^a		$\Phi_{\text{so}}^{\text{b}}$
Standard	ZnTPP ^b	0.73
Dyad	7	0.37
	8	0.31
	11	0.30
	13	0.34
Monomer	2	0.30
	16	0.32
	17	0.33
	15	0.32
	10	0.38

^aSee Figure 1 for structures

^bZnTPP Φ_{so} was taken as 0.73 from Ref. 31.

Conclusion

The chlorin-bacteriochlorin dyads which were newly synthesized in the present study reveal several interesting properties relevant to the FRET-imaging and PDT therapeutic applications. First, both the meso-aryl and β -pyrrole (position-3) substituted dyads reveal highly efficient FRET process with quantum yields approaching near unity, although such a process was slightly better for the β -pyrrole substituted derivatives due to shorter donor-acceptor distances. Second, the acceptor bacteriochlorin emission in the dyads is in the far-red region, a result relevant for deep-tissue imaging applications. Third, FRET measured from femtosecond transient absorption studies were found to be extremely efficient with rates on the order of 10^{11} s^{-1} . Forth, after completion of the FRET process, the $^1\text{Bchl}^*$ populated the $^3\text{Bchl}^*$ state by an intersystem crossing process. Finally, $^3\text{Bchl}^*$ interacted with dioxygen in solution to produce singlet oxygen with appreciable quantum yields. The present study brings out the significance of Chl-Bchl dyads as a new class of dual-functioning, i.e., FRET-imaging and therapeutic singlet oxygen producing agents. The *in vivo* imaging and long-term PDT efficacy studies of these compounds are underway.

Acknowledgments

Authors are thankful to the US National Cancer Institute (NCI), the Cancer Centre Support Grant CA016156 to the Roswell Park Comprehensive Cancer Centre (RPCCC), Buffalo, NY, the Roswell Park Alliance Foundation, Robert A. Welch Foundation (K.M.K., Grant E-680), and the National Science Foundation (Grant 2000988 to FD) for the financial support.

Conflict of interest

The authors declare no conflict of interest.

[1] a) S. He, J. Song, J. Qu, Z. Cheng, *Chem. Soc. Rev.* **2018**, *47*, 4258-4278. b) *Functional Dyes*, S.-H. Kim, Ed.; Elsevier: Amsterdam, Netherlands, 2006. c) J. Fabian, *Chem. Rev.* **1992**, *92*, 1197-1226.

- [2] a) D. Wu, L. Chen, W. Lee, G. Ko, J. Yin, J. Yoon, *Coord. Chem. Rev.* **2018**, *354*, 74-97. b) G. Li, Y. Y. Wei-Hsuan, *Nature Rev. Mater.* **2017**, *2*, 17043. c) J. Cui, Y. Li, L. Liu, L. Chen, M. Jun, F. Jingwen, G. Fang, E. Zhu, H. Wu, L. Zhao, L. Wang, Y. Huang, *Nano Lett.* **2015**, *15*, 6295-6301.
- [3] a) V. Bandi, H. B. Gobeze, F. D'Souza, *Chem. Eur. J.* **2015**, *21*, 11483-11494. b) V. Bandi, S. K. Das, S. G. Awuah, Y. You, F. D'Souza, *J. Am. Chem. Soc.* **2014**, *136*, 7571-7574. c) M. E. El-Khouly, S. Fukuzumi, F. D'Souza, *ChemPhysChem* **2014**, *15*, 30-47. d) A. Kamkaew, S. H. Lim, H. B. Lee, L. V. Kiew, L. Y. Chung, K. Burgess, *Chem. Soc. Rev.* **2013**, *42*, 77-88. e) H. Lu, J. Mack, Y. C. Yang, Z. Shen, *Chem. Soc. Rev.* **2014**, *43*, 4778-4823;
- [4] a) C.-C. Chen, L. Dou, R. Zhu, C. H. Chung, T. B. Song, Y. B. Zheng, B. Yue, S. Hawks, G. Li, P. A. Weiss, Y. Yang, *ACS Nano*, **2012**, *6*, 7185-7190. b) M. Zhu, X. Cai, M. Fujitsuka, J. Zhang, M. Junyong, T. Majima, *Angew. Chem. Int. Ed.* **2017**, *56*, 2064-2068. c) H. Kobayashi, M. Ogawa, R. Alford, P. L. Choyke, Y. Urano, *Chem. Rev.*, **2010**, *110*, 2620-2640.
- [5] a) M. Ethirajan, Y. Chen, P. Joshi, R. K. Pandey, *Chem. Soc. Rev.* **2011**, *40*, 340-362. b) P. P. Ghoroghchian, M. J. Therien, D. A. Hammer, *Nanomed. Nanobiotech.* **2009**, *1*, 156-167. c) C. Li, Q. Wang, *ACS Nano*, **2018**, *12*, 9654-9659. d) Q. Miao, K. Pu, *Adv. Mater.* **2018**, *30*, 1801778.
- [6] a) E. A. Owens, M. Henary, G. El Fakhri, C. Georges, H. S. Choi, *Acc. Chem. Res.* **2016**, *49*, 1731-1740. b) A. L. Vahrmeijer, M. Huttman, J. R. van der Vorst, C. J. H. van de Velde, J. V. Frangioni, *Nature Rev. Clinical Oncology*, **2013**, *10*, 507-518. c) S. A. Hilderbrand, R. Weissleder, *Curr. Opinion Chem. Biol.* **2010**, *14*, 71-79. d) J. V. Frangioni, *Curr. Opinion Chem. Biol.* **2003**, *7*, 626-634.
- [7] a) T. J. Dougherty, B. W. Henderson, G. Jori, D. Kessel, M. Korbelik, J. Moan, Q. Peng, *J. Natl. Cancer Inst.* **1998**, *90*, 889-905; b) P. Agostinis, K. Berg, K. A. Cengel, T. H. Foster, A. W. Girotti, S. O. Gollnick, S. M. Hahn, M. R. Hamblin, A. Juzeniene, D. Kessel, M. Korbelik, J. Moan, P. Mroz, D. Nowis, J. Piette, B. C. Wilson, J. Golab, *CA-Cancer J. Clin.* **2011**, *61*, 250-281. c) J. P. Celli, B. Q. Spring, I. Rizvi, C. L. Evans, K. S. Samkoe, S. Verma, B. W. Pogue, T. Hasan, *Chem. Rev.* **2010**, *110*, 2795-2838
- [8] a) S. G. Awuah, Y. You, *RSC Adv.* **2012**, *2*, 11169-11183; b) N. L. Oleinick, R. L. Morris, I. Belichenko, *Photochem. Photobiol. Sci.* **2002**, *1*, 1-21; c) T. J. Dougherty, *Semin. Surg. Oncol.* **1986**, *2*, 24-37. d) S. G. Awuah, S. K. Das, F. D'Souza, Y. You, *Chem. Asian J.* **2013**, *8*, 3123-3132. e) R. L. Watley, S. G. Awuah, M. Bio, R. Cantu, H. B. Gobeze, V. N. Nesterov, S. K. Das, F. D'Souza, Y. You, *Chem. Asian J.* **2015**, *10*, 1335-1343.
- [9] a) H. L. Kee, R. Nothdurft, C. Muthiah, J. R. Dieders, D. Fan, M. Ptaszek, D. F. Bocian, J. S. Lindsey, J. P. Culver, D. Holten, *Photochem. Photobiol.* **2008**, *84*, 1061-1072. b) K. Licha, *Top. Curr. Chem.* **2002**, *222*, 1-29. c) D. J. Hawrysz, E. M. Sevick-Muraca, *Neoplasia*, **2000**, *2*, 388-417. d) Y. Cakmak, S. Kolemen, S. Duman, Y. Dede, Y. Dolen, B. Kilic, Z. Kostereli, L. T. Yildirim, A. L. Dogan, D. Guc, E. U. Akkaya, *Angew. Chem. Int. Ed.* **2011**, *50*, 11937-11941; *Angew. Chem.* **2011**, *123*, 12143-12147.
- [10] J. Lakowicz, *Principles of Fluorescence Spectroscopy*, 3rd ed., Springer, Heidelberg, 2006.
- [11] a) C. Schweitzer, Z. Mehrdad, A. Noll, E.-W. Grabner, R. Schmidt, *J. Phys. Chem. A* **2003**, *107*, 2192-2198. b) B. Li, H. Lin, B. C. Wilson, *J. Biophotonics*, **2016**, *9*, 1314-1325. c) R. Schmidt, *Photochem. Photobiol.* **2006**, *82*, 1161-1177.
- [12] M. Kobayashi, M. Akiyama, H. Kano, H. Kise, *Spectroscopy and structure determination. In Chlorophylls and Bacteriochlorophylls: Biochemistry, Biophysics, Functions and Applications*, Ed. B. Grimm, R. J. Porra, W. Ru'diger, H. Scheer, pp. 79-94. Springer, Dordrecht, 2006, The Netherlands.
- [13] Limantara, L., P. Koehler, B. Wilhelm, R. J. Porra, H. Scheer, *Photochem. Photobiol.* **2006**, *82*, 770-780.
- [14] a) M. Ptaszek, B. E. McDowell, M. Taniguchi, H.-J. Kim, J. S. Lindsey, *Tetrahedron*, **2007**, *63*, 3826-3839. b) M. Taniguchi, M. Ptaszek, B. E. McDowell, J. S. Lindsey, *Tetrahedron*, **2007**, *63*, 3840-3849. c) M. Taniguchi, M. Ptaszek, B. E. McDowell, P. D. Boyle, J. S. Lindsey, *Tetrahedron*, **2007**, *63*, 3850-3863.
- [15] a) Y. Chen, G. Li, R. K. Pandey, *Curr. Org. Chem.* **2004**, *8*, 1105-1134. b) A. N. Kozyrev, Y. Chen, L. N. Goswami, W. A. Tabaczynski, R. K. Pandey, *J. Org. Chem.* **2006**, *71*, 1949-1960.

- [16] A. Kozyrev, M. Ethirajan, P. Chen, K. Ohkubo, B. C. Robinson, K. M. Barkigia, S. Fukuzumi, K. M. Kadish and R. K. Pandey, *J. Org. Chem.* **2012**, *77*, 10260-10271.
- [17] M. Ethirajan, P. Joshi, W. H. William III, K. Ohkubo, S. Fukuzumi and R. K. Pandey, *Org. Letters*, **2011**, *13*(8), 1956-1959.
- [18] R. K. Pandey, A. B. Sumlin, S. Constantine, M. Aoudia, W. R. Potter, D. A. Bellnier, B. W. Henderson, M. A. Rodgers, K. M. Smith and T. J. Dougherty, *Photochem. Photobiol.*, **1996**, *64*, 194-204.
- [19] H. Miyaura, A. Suzuki, *Chem. Rev.*, **1995**, *95*, 2457-2483.
- [20] W. Tang, A. G. Capacci, X. Wei, W. Li, A. Shite, N. Patel, J. Savole, J. J. Gao, S. Rodriguez, B. Qu, N. Haddad B. Z. Lu, D. Krishnamurthy, N. K. Yee, C. Senanayake, *Angew Chem. Int. Ed.* **2010**, *49*, 5879-5883.
- [21] B. Dayal, G. Salen, B. Toome, G. S. Tint, S. Shefer and J. Padia, *Steroids*, **1990**, *55*, 233-237.
- [22] N. Patel, P. Pera, P. Joshi, M. Dukh, W. A. Tabaczynski, K. E. Sifers, M. Kryman, R. Cheruku, F. Durrani, J. R. Missert, R. Watson, T. Y. Ohulchanskyy, E. C. Tracy, H. Baumann and R. K. Pandey, *J. Med. Chem.*, **2016**, *59*, 9774-9787.
- [23] H. Tamiaki, N. Hagio, S. Tsuzuki, Y. Cui, T. Zouta, X-F Wang, Y. Kinoshita, *Tetrahedron*, *74*, 4078-4085.
- [24] D. A. Hartzler, D. M. Niedzwiedzki, D. A. Bryant, R. E. Blankenship, Y. Pushkar, S. Savikhin, *J. Phys. Chem. B.* **2014**, *118*, 7221-7232.
- [25] P. G. Seybold, M. Gouterman, *J. Mol. Spectros.* **1969**, *31*, 1-13.
- [26] $\Phi_f = 0.033$ of zinc tetraphenylporphyrin in toluene was used as standard.
- [27] T. Förster, *Discuss. Faraday Soc.* **1959**, *27*, 7-17.
- [28] <http://www.fluortools.com/about>
- [29] D. Rehm, A. Weller, *Isr. J. Chem.* **1970**, *7*, 259-271.
- [30] a) S. K. Das, B. Song, A. Mahler, V. N. Nesterov, A. K. Wilson, O. Ito, F. D'Souza, *J. Phys. Chem. C* **2014**, *118*, 3994-4006. B) S. K. Das, A. Mahler, A. K. Wilson, F. D'Souza, *ChemPhysChem*, **2014**, *15*, 2462-2472.
- [31] G. Rossbroich, N. A. Garcia, S. E. Braslavsky, *J. Photochem.* **1985**, *31*, 37-48.

Received: ((will be filled in by the editorial staff))

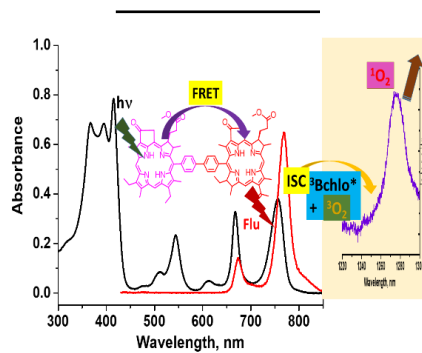
Revised: ((will be filled in by the editorial staff))

Published online: ((will be filled in by the editorial staff))

FRET into Far-IR Region

Meso and β -Pyrrole Linked Chlorin-Bacteriochlorin Dyads for Promoting Far-Red FRET and Singlet Oxygen Production

M. Dukh, W. A. Tabaczynski, S. Seetharaman, Z. Ou, K. M. Kadish,* F. D'Souza,* R. K. Pandey*



Far-IR FRET and singlet oxygen generating agents: A series of newly synthesized chlorin-bacteriochlorin dyads reveal efficient FRET emitting in the far-IR region useful for deep tissue imaging, and generates singlet oxygen desirable for photodynamic therapy applications.